Acta Polytechnica CTU Proceedings **33**:511–517, 2022
https://doi.org/10.14311/APP.2022.33.0511

Published by the Czech Technical University in Prague

EFFECT OF CRACKS ON THE SERVICE LIFE OF RC STRUCTURES EXPOSED TO CHLORIDES

Nicoletta Russo[a,*], Matteo Gastaldi[a], Luca Schiavi[b], Alberto Strini[b], Riccardo Zanoni[b], Federica Lollini[a]

[a] *Politecnico di Milano, Department of Chemistry, Materials and Chemical Engineering "Giulio Natta", Piazza Leonardo da Vinci 32, 20133 Milano, Italy*

[b] *Consiglio Nazionale delle Ricerche, Istituto per le Tecnologie della Costruzione, Viale Lombardia 49, 20098 San Giuliano Milanese, Italy*

[*] corresponding author: nicoletta.russo@polimi.it

Abstract. To move towards a more sustainable concrete, the enhancement of its durability is strongly encouraged and, dealing in particular with reinforced concrete (RC), this mainly means to prevent the damage due to environmental actions, e.g. due to chloride-induced corrosion. Therefore, there is the need of models aimed at designing durable structures. Usually the service life design models consider concrete in uncracked condition. In real structures, however, several phenomena can generate cracks on concrete surface, leading to an acceleration of the corrosion of steel rebar. A number of studies have been recently carried out in order to evaluate the influence of cracks on reinforced concrete durability in chloride-contaminated environment, however the knowledge of the effect of cracks on the initiation and propagation periods is still lacking. Furthermore, few studies have considered additional protection strategies, such as the use of stainless steel rebar. In this work, experimental results are presented concerning the influence of cracks on the service life of reinforced concrete structures in order to evaluate if cracks lead to an earlier corrosion initiation induced by chlorides. Prismatic specimens, reinforced with carbon steel and 304L stainless steel bars, were longitudinally cracked and exposed to ponding with 3.5% NaCl solution. The monitoring of corrosion behaviour showed that when cracks reached the steel surface corrosion initiated immediately.

Keywords: Corrosion initiation, Corrosion propagation, cracked concrete, chlorides, stainless steel.

1. Introduction

Nowadays the need of reducing the environmental impact of the construction industry, to increase its sustainability, is one of the main factors which guides the research and the innovation in the field of construction materials. An improvement in sustainability can be achieved by increasing the durability of RC structures, since the design stage.

To design durable structures several models have been developed, that allow to estimate the evolution in time of deterioration processes, and to evaluate the service life of a structure, as function of several parameters related both to material characteristics and to the environmental exposure conditions [1–3]. However, usually these durability models refer mainly to uncracked concrete, a condition that rarely occurs in practice. In real structures cracks on concrete surface can be generated by several phenomena: shrinkage, chemical reactions, mechanical loads, reinforcement corrosion, etc. Cracks are expected to inevitably form in RC structures, which in some cases develop as deep as the reinforcement, from the beginning of the life of the structure. The presence of cracks provides a more direct path for the ingress of chloride ions and oxygen into concrete, possibly leading to a reduction of the initiation time of steel corrosion and to an acceleration of the propagation of corrosion [4]. Some design codes provide, for structures subjected to aggressive exposure conditions, limitations in terms of crack opening at the concrete surface, in most cases in the order of magnitude of hundreds of micrometers, while studies on the durability of RC structures seem to show that there are effects even for much narrower cracks [5]. What is widely accepted from a structural point of view, therefore, may have significant consequences from the durability point of view, and, more in general, sustainability in the construction industry. The objective of the studies on the subject is to try to correlate the geometrical parameters of the cracks, in terms of crack surface opening and more rarely crack depth, with the consequences that these may have on corrosion initiation and propagation times, and therefore on the service life of structures.

Relative few studies, however, provide really useful information on the effects of cracks on chloride-induced corrosion of carbon steel bars and even fewer analyse more corrosion resistant bars such as stainless steel rebar, that can be used to increase the durability of RC structures exposed to chloride-bearing environment. Almost all these works refer to cracks formed in transverse direction with respect to the reinforcement and not in longitudinal direction [6]. Nevertheless, longitudinal cracks can be present in RC structures

Steel name	Mechanical properties			Main alloy elements [%]									
	US [MPa]	$YS_{0.2\,\%}$ [MPa]	A_{gt} [%]	C	Cr	Ni	Mo	Mn	N	Cu	Si	S	P	V
304L	760	543	24	0.021	18.51	8.61	0.15	1.31	0.146	-	-	-	-	-
CS	622	524	12.2	0.145	0.12	0.17	0.03	0.77	0.010	0.43	0.18	0.050	0.017	0.002

Table 1. Mechanical properties (US = ultimate strength; $YS_{0.2\%}$ = yield strength at 0.2% of deformation; A_{gt} = total elongation at maximum force) and main alloy elements of the stainless steel bars and carbon steel bars.

(e.g. in reinforced concrete bridge girders, in reinforced concrete pavements, due to loading or thermal shock, in steel reinforced concrete pipes, parking garage slabs [7]). Even structural cracks that tend to occur in transverse direction with respect to the flexural reinforcement, are parallel to the stirrups (shear reinforcement). As far as the Authors have been able to ascertain, the only studies that investigated the effect of natural longitudinal cracks (intended as induced by mechanical or thermal loading, as opposed to artificial notches) on the corrosion behaviour of carbon steel and stainless steel bars are [7, 8]. According to Poursaee and Hansson [7], the presence of longitudinal cracks, about 0.1 mm wide and as deep as the reinforcement, on concretes made with OPC (Ordinary Portland Cement) and HPC (High Performance Concrete), led to a shortened initiation time in comparison to sound concretes. In particular, after 128 weeks of exposure to salt, corrosion occurred on carbon steel bars embedded in OPC and HPC cracked concretes, whilst bars were still passive after 132 week of exposure when embedded in sound concretes. In Van Niejenhuis et al. [8], even with the use of stainless steel reinforcement, the initiation time was significantly reduced in presence of longitudinal cracks, characterized by average crack width between 0.13 mm and 0.53 mm (crack depth was not considered in this study). Since the presence of longitudinal cracks seems to strongly affect the durability of a RC structure, there is the need to carry out further studies on this topic.

An experimental research has been carried out in order to evaluate the effect of longitudinal cracks on concretes reinforced with carbon steel bars and 304L stainless steel bars. This paper reports the preliminary results obtained on the specimens exposed for about 13 months to ponding with a 3.5% sodium chloride solution.

2. Experimental procedure

Concretes were made with 422 kg/m^2 of Portland-Limestone Cement (PLC), type CEM II/A-LL 42,5R (according to EN 197-1), 190 kg/m^2 of water, w/c equal to 0.45, and 1731 kg/m^2 of calcareous aggregates, subdivided into five grain size fractions with a maximum diameter of 9 mm. An acrylic-based superplasticizer was also added to the mix, to increase workability. A S3 consistency class (according to EN 206) and an average compressive strength, on cubic specimens after 28 days of moist curing (R.H. $>$ 95%), of 51 MPa were obtained.

As reinforcement, 16-mm rebar in carbon steel (CS) and austenitic stainless steel (SS), of grade 304L, were used, mechanical properties and chemical compositions are reported in Table 1. The stainless steel bars were subjected to sand blasting and pickling from producers, in order to remove the oxide scale created during hot forming, whilst carbon steel bars were subjected to sand blasting in the laboratory. Before testing, after degreasing with acetone, the two ends of each bar were masked with a styrene-butadiene-modified cement mortar and coated with epoxy; a length of the bar of 80 mm was exposed to the concrete.

Prismatic specimens, with dimensions of $120 \times 90 \times 50$ mm, were reinforced with one steel rebar, with a concrete cover thickness of 15 mm, and equipped with an activated titanium wire (reference electrode) and a titanium wire (counter-electrode) for electrochemical measurements (Figure 1a). To account for the variability of the results, ten replicate specimens were made with each type of steel rebar. Five specimens for each type of steel were provided with a V-shaped notch, 5-mm depth, in the longitudinal direction on the casting surface, to promote the formation of a longitudinal crack. As a result, for each type of steel, five replicated specimens were tested in uncracked conditions and five in cracked conditions.

To obtain load-induced cracks, the day after casting, a sort of tree-point bending test was performed on specimens presenting the longitudinal notch, by means of a universal testing machine. The cracking procedure was not a crack width-controlled test, and, for some specimens, cracks were observed at the end of the exposure to chlorides. For further details, see [9].

All the reinforced specimens were wet cured (R.H. $>$ 95%) for 7 days. After the curing, a pond was fixed on the casting surface and a 3.5% NaCl solution was poured inside for approximately 13 months, with specimens kept in air-conditioned laboratory (T $\sim$ 20°C). The ponding was kept continuously for the first 6 months, with a monthly solution replacement, and subsequently wet and dry cycles were alternated

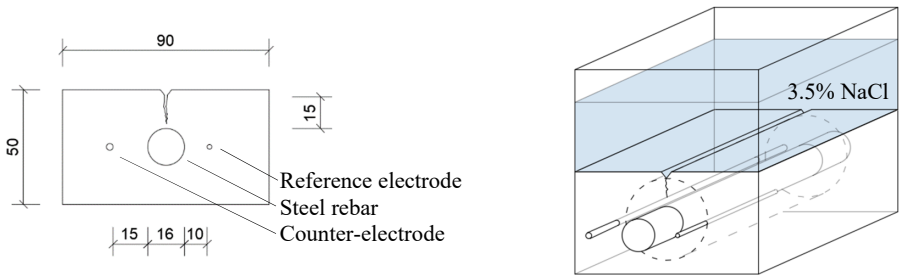

FIGURE 1. Geometry of the concrete specimens, dimensions in mm (a), and configuration of the ponding test and, in dotted line, concrete core taken for crack and corrosion observation (b).

(2 weeks dry, 1 week wet) to accelerate corrosion initiation, until about 400 days of total exposure. Before starting the wet/dry cycles, in order to estimate the chloride content at the rebar surface, powder samples at different depths from the exposed surface, 5 mm spaced and up to a depth of 25 mm, were collected by dry-drilling one of the uncracked specimens, and the chloride profile was measured by analysing the total chloride content (acid soluble).

During the whole exposure period, the corrosion of embedded steel bars was monitored by means of electrochemical measurements. Half-cell potential (E_{corr}) versus a saturated calomel electrode (SCE) was measured, placing the electrode on the specimen surface in correspondence of the central part of the rebar. Corrosion current density (i_{corr}) was measured through linear polarization resistance measurements (R_p) as

$$i_{corr} = \frac{B}{R_p \cdot A} \tag{1}$$

where A was the bar surface exposed to concrete and B was assumed equal to 26 mV. The measurements were periodically carried out at least with weekly frequency, except for the four months corresponding to the sanitary emergency related to COVID-19, during which the specimens were left at dry conditions in the laboratory.

In two out of five of the cracked specimens reinforced with carbon steel rebar, a reinforced concrete core (45 mm in diameter, parallel to the direction of the steel reinforcement) was drilled out of the specimen soon after corrosion initiation (Figure 1b). The core was then sawn, perpendicular to the direction of the steel reinforcement, in different segments. Each segment was polished and observed with a stereomicroscope, to investigate the crack pattern and to detect the presence of corrosion attack at the steel/concrete interface. Moreover, also the casting surface of the cracked specimens was observed with the stereomicroscope, after six months of exposure, to quantify the crack width.

3. Results and discussion

The monitoring of corrosion potential (E_{corr}) and corrosion current density (i_{corr}) of the bars started from the beginning of the exposure to ponding with a chloride solution. Figures 2 and 3 show the trend in time of corrosion potential and corrosion current density of carbon steel and 304L stainless steel bars embedded in all replicate uncracked and cracked concrete specimens. In the Figures, the black symbols indicate the corrosion current density, whilst the grey symbols indicate the corrosion potential.

With regard to the carbon steel bars embedded in uncracked concrete specimens (Figure 2a) at the beginning of the exposure to ponding, E_{corr} around -150 mV vs SCE and i_{corr} around 1 mA/m^2 for all the bars were measured, suggesting the passivation of the steel bars. During the continuous ponding exposure period, a slight increase of E_{corr} and a decrease of i_{corr} occurred on all the carbon steel bars embedded in uncracked concretes, reaching values around $-30 \div -50$ mV vs SCE for the corrosion potential and $0.7 \div 0.8$ mA/m^2 for the corrosion current density after about 180 days of exposure. These values suggested that passive conditions were maintained in time on all the rebar despite the penetration of chloride ions due to the exposure to ponding. In order to accelerate corrosion initiation, wet/dry cycles with the same solution were started. During the cycles, the electrochemical conditions changed for two out of five rebar. For one bar after the first wet cycle (218 days of exposure) and for the other during the third wet cycle, performed after the COVID-19 suspension (384 days). A sharp decrease of E_{corr} to -250 mV vs SCE and increase in i_{corr}, to about 1.5 mA/m^2 were experienced, clearly indicating the initiation on corrosion. For the other three CS bars in uncracked specimens, after about 400 day of exposure E_{corr} was around -100 mV vs SCE (up to around -20 mV vs SCE soon after the COVID-19 suspension) and i_{corr} around 1 mA/m^2 suggesting that passive conditions were maintained.

As it concerns the cracked concrete specimens reinforced with carbon steel bars (Figure 2b), at the beginning of the exposure to ponding the corrosion potential of 4 out of 5 bars was around -150 mV vs

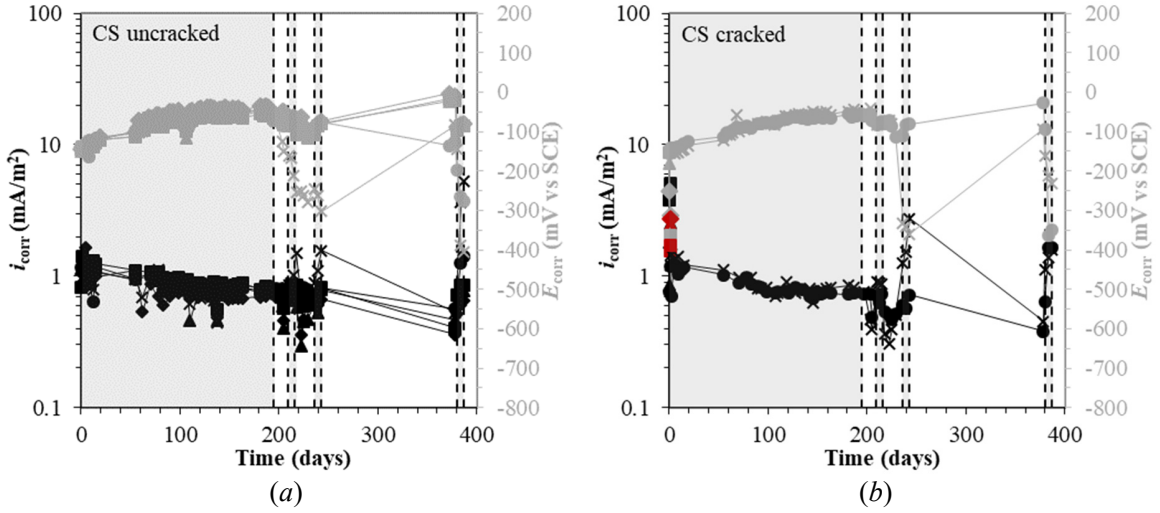

Figure 2. Evolution in time of the corrosion potential (grey symbols) and corrosion current density (black symbols) of carbon steel bars embedded in the five replicate uncracked (a) and cracked (b) concretes and exposed to ponding with a 3.5% NaCl solution; red symbols in (b) corresponding to the interruption of exposure for corroding specimens.

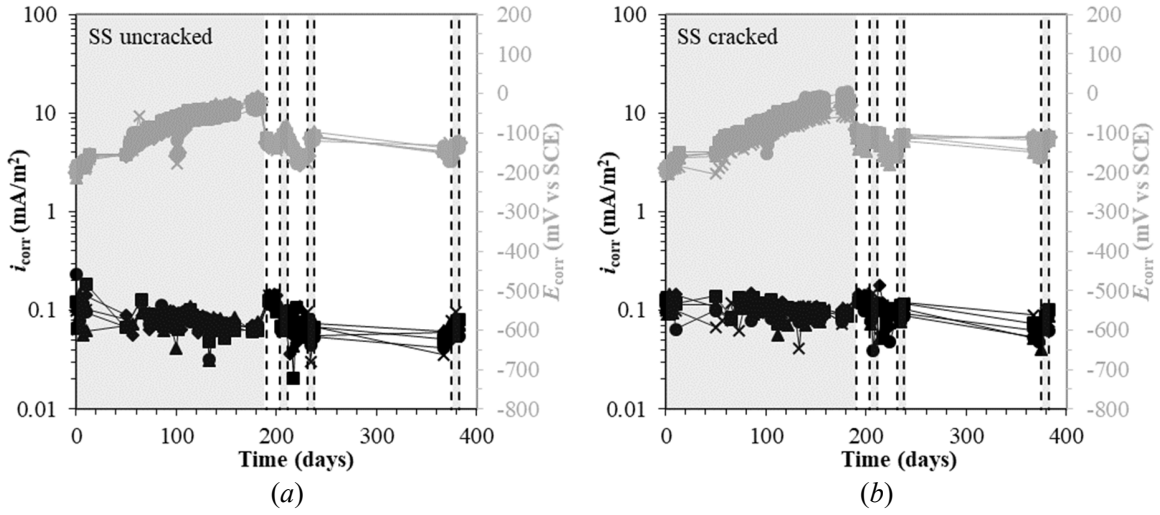

Figure 3. Evolution in time of the corrosion potential (grey symbols) and corrosion current density (black symbols) of 304L stainless steel rebars embedded in the five replicate uncracked (a) and cracked (b) concretes and exposed to ponding with a 3.5% NaCl solution.

SCE and the corrosion current density was around 1 mA/m^2, whilst E_{corr} of one bar was -250 mV vs SCE and i_{corr} was 1.5 mA/m^2. Few hours after the beginning of ponding, E_{corr} of this bar dropped to values lower that -300 mV vs SCE and i_{corr} increased up to values higher than 2.5 mA/m^2. Also the corrosion potential of two other bars experienced a drop after few hours from the beginning of the exposure, as well as the corrosion current density increased. The corrosion behaviour observed on these three bars suggested that corrosion initiated immediately. The ponding was then interrupted in these specimens (last measurements in red in Figure 2b). In the other two cracked specimens (Figure 2b), after the first six months of continuous ponding E_{corr} resulted around -50 mV vs SCE and i_{corr} around 0.8 mA/m^2, in accordance with values detected on the uncracked specimens, indicating that passive conditions were maintained despite chloride penetration. Both the remaining specimens, however, started corroding during the exposure to wet/dry cycles, one during the second dry cycle (236 days of exposure), the other during the third wet cycle (384 days), experiencing a drop in E_{corr}, to values around -350 mV vs SCE and a rise in i_{corr}, up to 2.7 mA/m^2.

The corrosion behaviour of stainless steel bars embedded in uncracked and cracked specimens is shown in Figure 3a and 3b, respectively. It can be observed that the corrosion potential slightly increased and the corrosion current density slightly decreased during the continuous ponding in all the bars embedded both in uncracked and cracked concrete. The corrosion potential was around $-50 \div 0$ mV vs SCE after about six months of exposure, whilst the corrosion current den-

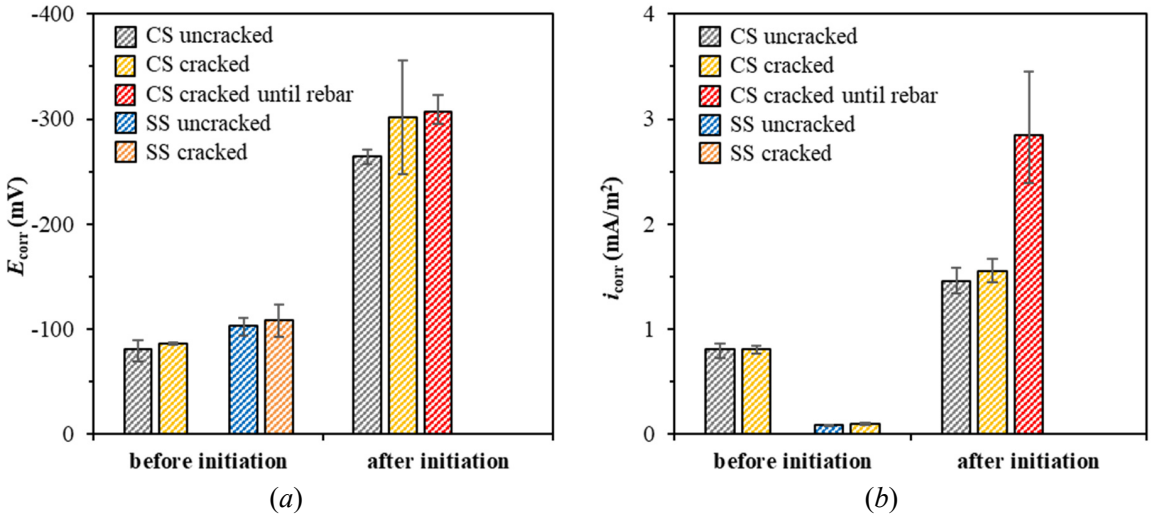

FIGURE 4. Average values of the corrosion potential (a) and corrosion current density (b) before and after initiation of corrosion for all the replicate specimens.

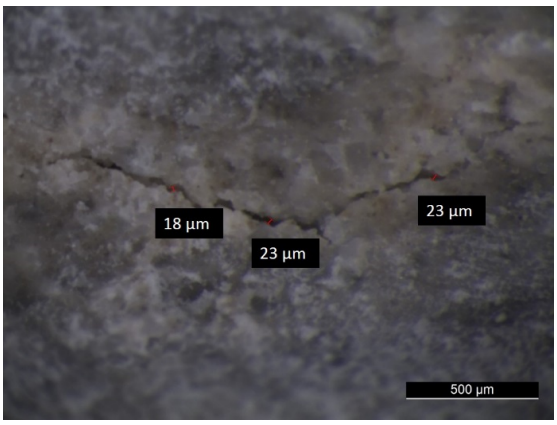

FIGURE 5. Microscopic image of the exposed surface on a cracked specimen after six months of exposure to ponding.

FIGURE 6. Microscopic image of polished cross section from a cracked specimen reinforced with CS bar, after corrosion initiation.

sity was of about 0.1 mA/m^2 without any significant difference among replicate specimens and in presence of longitudinal cracks. Also the exposure to wet/dry cycles did not significantly affect the electrochemical measurements on stainless steel rebar. In spite of the penetration of chlorides in time due to ponding and wet/dry cycles with NaCl solution and the expected increase of the amount of the chlorides near the bars, corrosion did not occur on the 304L stainless steel rebar, neither in sound nor in cracked conditions.

To summarize, as it concerns sound specimens, no corrosion occurred during the six months of continuous exposure to ponding with a sodium chloride solution neither in specimens reinforced with CS bars nor in those with SS bars. With the starting of wet and dry cycles, two specimens reinforced with CS started corroding, whilst other three maintained passive conditions up to 387 days of exposure. Therefore, initiation time (t_i) can be considered quite variable, included in the range 218 days and $>$ 387 days. This high variability is typical of chloride induced corrosion, since for the same concrete cover thickness, initiation time is related to the critical chloride threshold (Cl_{th}), which is characterized by a stochastic nature, and to the variability of the apparent diffusion coefficient of chlorides for different specimens. The influence of the latter parameter, however, is of minor extent, since tests performed to evaluate the resistance to chloride penetration on specimens with the same geometry and composition showed a good repeatability of results [9]. As it concerns the Cl_{th}, in order to have an indication of the expected chloride content at the steel surface after about six months of exposure to continuous ponding and just before the initiation of wet/dry cycles, powder samples were collected from one of the uncracked specimens. From titration of powder samples, the estimation of the chloride content at the bars depth, resulted 1.2% and 0.08% vs mass of cement, in correspondence of the top and bot-

tom side, respectively. According to [3], for carbon steel bars, Cl_{th} is included in the range $0.2 - 2\%$ by mass of cement, and in fact, one CS rebar started corroding soon after the evaluation of chloride content, another one after two further wet/dry cycles. On the other hand, Cl_{th} of 304L stainless steel, according to the literature, is higher than 3.5% by mass of cement [10], therefore it is reasonable to consider that the amount of chlorides at rebar depth is still well below Cl_{th} even after about 400 days of exposure.

For cracked specimens, initiation time is influenced also by the presence of the crack, a discontinuity in the concrete cover that promotes the penetration of chlorides towards the rebar. The geometrical parameters of the crack, therefore, should be considered as further variables affecting t_i. In this study, in cracked specimens reinforced with CS bars, corrosion initiated as soon as the ponding started in three out of five specimens, while corrosion initiated after months of exposure to chlorides ($236 < t_i < 384$ days) in the other two replicate specimens. This difference in behaviour could be attributed to differences in the obtained crack in different specimens, therefore an investigation on crack geometrical parameters, in terms of crack width and crack depth, was performed.

Crack width was observed on the exposed surface and after 6 months of exposure on the two cracked specimens still under testing. A clear detection of the crack along the whole specimens was difficult, maybe due to the presence of crystallized salt on the surface, or to self-healing phenomena that might have occurred during the ponding exposure. Where the crack was clearly visible, a width around 20 μm was measured (Figure 5).

It is worth to mention however that, even if in most literature studies only crack width is considered (typically during the cracking procedure, by means of linear variable displacement transducers, LVDTs), this could be misleading. In previous studies, in fact, a clear correlation between crack width and crack depth was not clearly defined and variation of cracks parameters along the specimens was detected [9]. Therefore, also crack depth was investigated in this study, through destructive tests on the three specimens that started corroding immediately (as described in Paragraph 2). Figure 6 shows, as an example, a wide field image obtained combining three different microscope images at 6× of magnification. It can be observed that the crack was characterized by a depth higher than the concrete cover thickness. In several observed sections the crack was at least equal to the concrete cover. A crack width in correspondence of the exposed surface of the order of 15-20 μm was measured on these specimens (comparable with values measured on cracked specimens where corrosion had not initiated immediately). In the section where the crack arrived until rebar depth, corrosion was detected.

In CS specimens where the crack developed until the rebar, corrosion started almost immediately after the exposure to a chloride solution, therefore t_i was almost equal to zero. On the other hand, in the cracked specimens where corrosion initiated months after the exposure to chlorides, it may be supposed that the crack did not develop until rebar depth. In this case, the results obtained seem to indicate that t_i was statistically reduced by the presence of the crack, since up to 387 days of exposure, both cracked samples showed corrosion initiation, while in the uncracked conditions, corrosion initiation started only on two out of five samples). However, the number of samples tested was limited, and therefore further investigation of this aspect is required. Moreover, it is reasonable to assume that also in the case of cracked specimens reinforced with SS rebar crack developed until rebar depth in some of the specimens. From results of this study, however, SS rebar remained in passive conditions, independently from crack parameters, for about 400 days after the exposure to chlorides.

On uncracked specimens and cracked specimens reinforced with CS that experienced corrosion during the wet and dry cycles with NaCl, the exposure was not interrupted as soon as corrosion initiated, in order to investigate the propagation period. Figure 4a and 4b, show, respectively, the average values of corrosion potential and corrosion current density, before and after initiation time.

It can be noted that no particular differences in corrosion potential were detected, for CS in uncracked and cracked configurations, both before and after corrosion initiation. On the other hand, corrosion current density resulted affected by the presence of the crack in the case the crack developed until rebar depth, being almost doubled with respect to sound and slightly cracked configurations.

It must however be noted that chloride induced corrosion is characterized by localized attacks (pitting), and that the linear polarization resistance technique gives a corrosion rate averaged on the whole steel surface. A higher corrosion current density, therefore, may be representative of a wider surface of steel affected by corrosion, but not the most severe condition in terms of loss of resistant cross section in time. Further investigation will be required on carbon steel bars to have better statistical results related to initiation time in the different configurations, and destructive test will be performed some months after corrosion initiation for both the steel types in cracked configuration, to observe the crack and the morphology of corrosive attacks (also in uncracked samples to evaluate the corrosion propagation).

4. Conclusions

Corrosion tests were carried out on concrete specimens reinforced with carbon steel and 304L stainless steel bars, in sound and longitudinally cracked configurations, with crack width at the exposed surface

around 20 μm. Specimens were exposed to a 3.5% NaCl solution, by means of continuous ponding for the first six months and subsequently to wet and dry cycles up to about 400 days of exposure.

In uncracked configuration, only two out of five specimens reinforced with carbon steel bars started corroding, with variable initiation time (>218 days) and the variability was reasonably attributed to the stochastic nature of pitting corrosion initiation.

In cracked configuration, all the carbon steel rebar started corroding, showing two different behaviours. For three specimens out of five, where the crack was observed to develop until rebar depth, corrosion started immediately after the exposure to ponding (corrosion initiation time equal to zero). A higher initiation time ($236 < t_i < 384$ days) was detected for the other two specimens, for which it was reasonably supposed that the crack did not develop until rebar depth. Thus, corrosion initiation seemed to be statistically shortened with respect to sound configuration, likely due to the promotion of chloride penetration into the crack. Nevertheless, the average values of corrosion potential and corrosion current density before and after corrosion initiation were comparable, suggesting that cracks did not affect corrosion process. Finally, stainless steel bars in uncracked and cracked specimens were still in passive conditions after about 400 days of exposure, due to the higher critical chloride threshold. Therefore, stainless steel resulted to have a high resistance to corrosion also in cracked configuration, even in the possible case in which crack developed until rebar depth.

References

[1] fib.Durable concrete structures Bulletin No. *183*, 1992.

[2] Duracrete. Probabilistic performance based durability design of concrete structures. Final Technical Report of Duracrete project, 2000. https://cordis.europa.eu/project/id/BRPR950132.

[3] fib. Model Code for Service Life Design Bulletin no. *34*, 2016.

[4] A.C. Boschmann Käthler, U. M. Angst, M. Wagner, et al.. Effect of cracks on chloride induced corrosion of steel in concrete - a review. NPRA reports Norwegian Public Roads Administration, 2017.

[5] I.-S. Yoon, E. Schlangen. Experimental examination on chloride penetration through micro-crack in concrete. *KSCE Journal of Civil Engineering* **18**(1):188-98, 2013. https://doi.org/10.1007/s12205-014-0196-9.

[6] F. U. A. Shaikh. Effect of Cracking on Corrosion of Steel in Concrete. *International Journal of Concrete Structures and Materials* **12**(1), 2018. https://doi.org/10.1186/s40069-018-0234-y.

[7] A. Poursaee, C. M. Hansson. The influence of longitudinal cracks on the corrosion protection afforded reinforcing steel in high performance concrete. *Cement and Concrete Research* **38**(8-9):1098-105, 2008. https://doi.org/10.1016/j.cemconres.2008.03.018.

[8] C. B. Van Niejenhuis, S. Walbridge, C. M. Hansson. The performance of austenitic and duplex stainless steels in cracked concrete exposed to concentrated chloride brine. *Journal of Materials Science* **51**(1):362-74, 2015. https://doi.org/10.1007/s10853-015-9387-0.

[9] N. Russo, M. Gastaldi, P. Marras, et al. Effects of load-induced micro-cracks on chloride penetration resistance in different types of concrete. *Materials and Structures* **53**(6), 2020. https://doi.org/10.1617/s11527-020-01580-y.

[10] F. Lollini, M. Carsana, M. Gastaldi, and E. Redaelli. Corrosion behaviour of stainless steel reinforcement in concrete. *Corrosion Reviews* **37**(1):3-19, 2019. https://doi.org/10.1515/corrrev-2017-0088.